ISSN 0915-633X

NATIONAL INSTITUTE FOR FUSION SCIENCE

Effects of a Nonuniform Open Magnetic Field on the Plasma Presheath

K. Sato and F. Miyawaki

(Received – Nov. 29, 1990)

NIFS-67 Jan. 1991

RESEARCH REPORT
NIFS Series

NAGOYA, JAPAN

Effects of a nonuniform open magnetic field on the plasma presheath

Kunihiro Sato and Fujio Miyawaki

Department of Electrical Engineering,

Himeji Institute of Technology,

Himeji 671-22, Japan

ABSTRACT

Effects of a nonuniform magnetic field on the plasma presheath is numerically investigated using the plasma equation for a collisionless plasma with a finite-temperature particle source. The present calculation confirms that previously published analytical solutions [Phys. Fluids B 1, 725 (1989)] are available over a wide range of mirror ratio. Potential drop in the presheath, which considerably depends on both the magnetic strength profile and the spatial distribution of the particle source, is remarkably increased by applying an expanding magnetic field when plasma particles are generated in the inner part of the plasma. An effect of a nonuniform magnetic field on sheath formation is also discussed by using the calculated ion distribution function. If the plasma equation has no singularity at the sheath edge, its solution satisfies the generalized Bohm criterion with the inequality sign in the expanding magnetic field.

Keywords; presheath, open field plasma, expanding magnetic field, sheath, Bohm criterion

I. INTRODUCTION

The problem of the potential formation in a plasma in contact with a wall is important for research on magnetically confined plasmas as well as on the plasma source used in plasma processing. Potential developed in a plasma flowing along a nonuniform open magnetic field becomes an issue when we approach the subject of the plasma flow, energy transport, an inflow of high-Z impurity ions, and plasma-surface interactions in an open region of confinement systems. In the presence of an expanding magnetic field, ions are accelerated toward the plate and their density drops accordingly. If electrons remain close to a Maxwellian distribution then the electrostatic potential will increase following the Boltzmann relation. Accelerated ions will also facilitate formation a shielding positive space charge at the plasma boundary. Therefore, the expanding magnetic field is expected to be available for enlargement of the potential along a field line and stabilization of the sheath potential.

The problem of plasma flow to a wall and the potential formation has drawn attention since the first kinetic analysis in the context of discharge plasmas was done by Tonks and Langmuir[1]. Progress on the theoretical treatment of this problem has been made by a number of workers over many years[2–4]. In the previous analyses the plasma is either unmagnetized or magnetized by a uniform field.

Recently, Sato et al. formulated the plasma-sheath equation for a collisionless plasma with a finite-temperature particle source in an expanding magnetic field[5], in which the same ion source function used by Emmert et al. is adopted and Boltzmann electrons is assumed. They obtained an analytic solution by introducing some simplifying ap-

proximations and presented the potential profile, the potential at the sheath edge, and the wall potential as well as the particle and energy fluxes to the sheath for different magnetic mirror profiles. Hussein et al. numerically simulated the same plasma and investigated the dependence of the presheath potential on both the spatial distribution of the particle source and the magnetic field strength profiles[6]. They compare the simulation results with the analytical solution obtained by Sato et al., showing that the simulation results agree well with Sato et al. for low mirror ratios but deviate as the mirror ratio increases. Although they concluded that the differences between them is attributed to the approximation made in the analysis, the differences mainly originate in a particle source used in the analysis and in the simulation. A particle source used in the analysis has a spatial profile in proportion to the plasma particle density but that in the simulation has a uniform spatial profile .

In this paper, we numerically studied potential formation in the plasma immersed in a nonuniform magnetic field by solving the plasma equation formulated previously. We compare the numerical results with the analytical ones and also with the simulation ones to show justice of approximations in the analysis carried by Sato et al. and to check accuracy of the simulation code developed by Hussein et al.. Moreover, we investigated the dependence of the potential profile on spatial distribution of the particle source and show upper and lower limits of the potential drop in the presheath to indicate controlability of the presheath potential by applying an expanding magnetic field. We also discuss an effect of the nonuniform magnetic field on sheath formation using the calculated ion distribution function.

In Sec. 2, we describe the model and write the plasma equation. An effect of a nonuniform magnetic field on sheath formation is briefly discussed in Sec. 3. The numerical results are presented and discussed in Sec. 4, and the conclusions are given in Sec. 5.

II. MODEL AND PLASMA EQUATION

The model and coordinate system used throughout this paper is illustrated in Fig. 1. The collisionless plasma contained between two perfectly absorbing walls located at $x = \pm L$ is symmetric about $x = 0$. The Debye length is assumed to be small compared with macroscopic scale length, and then quasineutrality along field lines holds true over the whole region except the sheath region.

Using the energy ε and the magnetic moment μ, the kinetic equation for ions is simply described by

$$\sigma v_{\parallel}(x,\varepsilon,\mu)\frac{\partial f(x,\varepsilon,\mu,\sigma)}{\partial x} = S(x,\varepsilon,\mu), \tag{1}$$

where

$$v_{\parallel}(x,\varepsilon,\mu) = \left\{2\left(\varepsilon - \mu B(x) - q\Phi(x)\right)/M\right\}^{1/2} \tag{2}$$

is the speed of ion along the field line, $\sigma(=\pm 1)$ denotes the direction of the ion motion, $f(x,\varepsilon,\mu,\sigma)$ is the ion distribution function, $S(x,\varepsilon,\mu)$ is the source term for the ions, M is mass, q is the ion charge, $\Phi(x)$ is the electrostatic potential, and $B(x)$ is the magnetic field strength. The ion source used by Emmert et al. is expressed in the form

$$S(x,\varepsilon,\mu) = S_0 h(x)\frac{M^2}{4\pi(kT_i)^2}v_{\parallel}(x,\varepsilon,\mu)\exp\left\{\frac{-(\varepsilon - q\Phi(x))}{kT_i}\right\} \tag{3}$$

where S_0 is the source strength, k is Boltzmann's constant, T_i is the source temperature, and $h(x)$ expresses the spatial distribution of the source. The distribution function $f(x, \varepsilon, \mu, \sigma)$ is obtain by integrating Eq. (1) along the trajectory of ions using the boundary conditions $f(-L, \varepsilon, \mu, +1) = 0$ and $f(L, \varepsilon, \mu, -1) = 0$. Ion density $n_i(x)$ is calculated by integrating the distribution function over the $\varepsilon - \mu$ space.

Since the electrons are in a retarding electrostatic potential, the electrons can be assumed to have a Boltzmann distribution with temperature T_e. Results of particle simulation shows that the bulk of electrons approaches to the Boltzmann distribution ever if the mean free path is much larger than the scale length of a plasma[7]. We can equate ion and electron charge densities in the presheath region to obtain the the plasma equation. Introducing the nondimensional variables

$$\Psi(s) = -e\Phi(s)/kT_e, \quad R(s) = B_0/B(s), \quad s = x/L, \quad Z = q/e,$$

and

$$\tau = T_e/T_i \ ,$$

we describe the plasma equation derived by Sato et al. in the form

$$n_0 \exp(-\Psi(s)) = Z S_0 L \left(\frac{\pi M}{2kT_i}\right)^{1/2} \int_0^1 ds' G(s, s') h(s') \tag{4}$$

where

$$G(s, s') = \begin{cases} \exp\{Z\tau(\Psi(s) - \Psi(s'))\}\mathrm{erfc}\{Z\tau(\Psi(s) - \Psi(s'))^{1/2}\} \\ \quad - \left(\frac{R(s)-R(s')}{R(s)}\right)^{1/2} \exp\left(\frac{R(s)}{R(s)-R(s')} Z\tau(\Psi(s) - \Psi(s'))\right) \\ \quad \times \mathrm{erfc}\left\{\left(\frac{R(s)}{R(s)-R(s')} Z\tau(\Psi(s) - \Psi(s'))\right)^{1/2}\right\} \ , & s' < s \\ \\ \exp\{Z\tau(\Psi(s) - \Psi(s'))\} \ , & s' \geq s \ . \end{cases}$$

The electrostatic potential in the presheath is obtained by solving Eq. (4) and the wall potential Ψ_w also determined from the requirement of equal ion and electron fluxes to the wall.

III. EFFECT ON SHEATH FORMATION

The Sheath is assumed to be so thin that the particle source and variation of the magnetic field strength can be neglected inside the sheath. The solution of the plasma equation satisfies quasineutrality at the sheath edge and the particle flux is conserved in the sheath. Using quasineutrality in the plasma and conservation of the particle flux in the sheath, we can derive the relation

$$< V_{\|}^{-2} > \; = \; \frac{2}{Z^2} + \frac{2}{Z} \frac{dR/ds}{d\Psi/ds} \frac{\partial (n_i/n_1)}{\partial R}\bigg|_{s=1}, \tag{5}$$

where $V_{\|} = (MV_{\|}^2/2kT_e)^{1/2}$ is the normarized parallel velocity and the brackets $< >$ denote averaging with the ion distribution function[5]. The second term of rhs of Eq. (5) describes an effect of the nonuniform magnetic field. When the magnetic field is expanding, that is $dR/ds > 0$, the plasma equation for any source function satisfies the generalized Bohm criterion,

$$< V_{\|}^{-2} > \; \leq \; \frac{2}{Z^2}, \tag{6}$$

because the derivative $\partial n_i/\partial R$ in Eq. (5) is always negative at the sheath edge. The equality in Eq. (6) is true when the magnetic field is uniform or the field singularity

appears at the sheath edge[8]. Appearance of the field singularity depends on both the spatial distribution and the velocity distribution of the particle source. If there is no particle source in the vicinity of the sheath edge or the particle source has no ions with zero parallel speed like Emmert's source, the field singularity does not appears and the derivative $d\Psi/ds$ has a finite value. In this case the generalized Bohm criterion is fulfilled with the inequality sign. Oversatisfaction of the Bohm criterion is favorable for formation of a shielding positive space charge at the plasma boundary and then one can expect that an expanding magnetic field has a stabilizing effect of the sheath potential.

IV. RESULTS AND DISCUSSION

For the purpose to demonstrate effects of the expanding magnetic field on the presheath potential, we now solve the plasma equation which is the nonlinear integral equation. This equation can be solved numerically by transforming it into a set of finite difference equations. We can obtain the numerical solution with a high accuracy better than 10^{-5} by iterating on the potential until it converges. We express the model field $R(s)$ as a function of the coordinate s and assume the temperature of ion T_i to equal the electron temperature T_e.

At first, to show justice of simplifying approximations in the analysis carried by Sato et al. and to check accuracy of the simulation code developed by Hussein et al., we compare the calculation results with the analytical ones and the simulation ones. Figure 2 shows the potential profile in the presheath of a collisionless hydrogen plasma flowing along a magnetic field with a magnetic mirror profile used by Sato et al.. Different two

spatial profiles of the particle source generate different potential profiles. The dotted lines are the values computed by Sato et al. for the particle source with the spatial distribution $h(s) = n(s)/n_0$ and broken lines are the simulation result by Hussein et al. for the particle source with $h(s) = 1$. The difference between the analytical solutions and the numerical results is smaller than two percent. The simulation results also agrees well with the numerical ones but deviate near the sheath edge. The difference seems to be attributed to construction of a numerical grid introduced in their simulation. Fig. 3 shows the dependence of the potential at the sheath edge Ψ_1 and that at the wall Ψ_w on the mirror ratio R_1. Excellent agreement between the numerical results and the analytical solution within two percent is obtained over the wide range of the mirror ratio; the difference is within two percent over the range of R_1 from 1 to 10. Some difference is observed between numerical results and simulation results, which is considered mainly to be an error due to the technic applied in the simulation. Hussein et al. have concluded that the differences between Sato et al.'s results and theirs are attributed to the approximations made in the analysis in Ref. 5, comparing their simulation results with the analytical solution. We, however, can see from Figs. 2 and 3 that these differences are mainly due to the different spatial profile of the particle source.

The dependence of the electrostatic potential and the particle density on the magnetic mirror ratio is illustrated in Figs. 4 and 5, where the spatial profile of the particle source is given by the Gaussian like that $h(s) = \exp(-25s^2)$. The parabolic profile of the magnetic mirror ratio given by $R(s) = 1 + (R_1 - 1)s^2$ is used heretofore. In the case of a constant magnetic field the potential changes only over the source region and is

constant elsewhere. Upon applying the expanding magnetic field, the potential continues to vary in the sourceless region. The potential drop increases with increasing of the edge magnetic mirror ratio R_1. Figure 6 shows the ion distribution function at the sheath edge for various magnetic mirror ratios. The expanding magnetic field accelerates the plasma toward the wall and then the plasma is predicted to satisfy a condition for sheath formation at the sheath edge. The value of $< V_{\|}^{-2} >$ calculated from the ion distribution function is equal to 2.0 in the uniform magnetic field and it becomes smaller than 2.0 in the presence of the nonuniform magnetic field. Then the generalized Bohm criterion is satisfied with the inequality sign in the expanding magnetic field. The value of $< V_{\|}^{-2} >$ also is checked to agree the value calculated from Eq. (5). From these results we can expect that the expanding magnetic field have a stabilizing effect on sheath formation.

In the presence of the nonuniform magnetic field the potential drop in the presheath considerably depends on the spatial distribution of the particle source. Figures 7 and 8 illustrate the dependence of the potential and the particle density on the spatial distribution of the particle source. The calculation is carried for three typical spatial distributions. In the case of the particle source near the plate, the potential is only developed over the region where the particle source exists and the magnetic field inside the particle source has no effect on potential formation. This can be seen from Eq. (4) in which the integrand G is independent of the magnetic mirror ratio when $s' \geq s$. In this case the only magnetic field in the source region affects the potential formation. On the contrary, in the case of the particle source near the center, the potential is developed not only over the source region but also over the sourceless region. The potential development in

the sourceless region is the result of the expansion of the magnetic flux tube. Figure 9 shows the ion distribution at the sheath edge for various spatial profiles of the particle source. The plasma flow velocity at the sheath edge exceeds the ion sound velocity and the generalized Bohm criterion is fulfilled with the inequality sign.

From results shown in Fig. 7 we can predict that the potential Ψ_1 has the maximum value when the particle source is concentrated at the center and has the minimum value when the particle source is localized near the wall. The maximum value is independent of the mirror ratio profile but dependent on the mirror ratio at the sheath edge R_1. Figure 10 shows the dependence of the upper and lower limits of potentials Ψ_1 and Ψ_w on the mirror ratio R_1. The region bounded by these limits show the region in which we can control the presheath potential by changing the mirror ratio and the profile of the magnetic field. Broken lines are results for the particle source with $h(s) = 1$. One can also see that the wall potential increases gradually but the potential drop in the sheath decreases slightly with the mirror ratio. Results in Figs. 7 and 10 show that we can effectively control the presheath potential by applying the expanding magnetic field with an adequate mirror ratio profile.

V. CONCLUSIONS

We have investigated formation of the presheath potential in the presence of an expanding magnetic field by numerically solving the plasma equation for the collisionless plasma. We have checked validity of the analysis and accuracy of the simulation code by

comparing the present calculation results with a previously published analytical solution and recently published simulation results. Results show that analytical solutions obtained by Sato et al. are available over a wide range of the mirror ratio, and the present result of the potential profile also agrees with the simulation result obtained by Hussein et al. except the region near a wall.

We have studied the dependence of the presheath potential profile on the spatial profile of the particle source and that of the magnetic field strength. Results show that a particle source profile has a considerable effect on the potential drop in the presence of a nonuniform magnetic field. If a plasma source exists in the interior of the plasma, we can effectively enlarge the potential drop in the presheath by increasing the magnetic mirror ratio. We have shown the upper and lower limits of the presheath potential as a function of the magnetic mirror ratio. The potential drops can be controlled within these limits by applying an expanding magnetic field with a proper field strength profile.

We have discussed an effect of a nonuniform magnetic field on sheath formation by calculating the ion distribution function. The plasma is accelerated by the gradient of the magnetic field strength and the plasma flow velocity at the sheath edge exceeds the sound velocity. The plasma flow in the presence of the expanding magnetic field satisfies the generalized Bohm criterion with the inequality sign if the sheath edge does not exhibit the the singularity.

ACKNOWLEDGEMENTS

The authors wish to thank Yoshiki Ikeda for his considerable assistance in the numerical calculation.

REFERENCES

[1]L. Tonks and I. Langmuir, Phys. Rev. **34**, 876 (1929).

[2]E. R. Harrison and W. B. Thompson, Proc. Phys. Soc. London **74**, 145 (1959).

[3]G. A. Emmert, R. Wieland, A. Mense, and J. Davidson, Phys. Fluids **23**, 803 (1980).

[4]R. C. Bissel and P. C. Johnson, Phys. Fluids **30**, 779 (1987)

[5]K. Sato, F. Miyawaki, and W. Fukui, Phys. Fluids B **1**, 725 (1989).

[6]M. A. Hussein and G. A. Emmert, Phys. Fluids B **2**, 218 (1990).

[7]T. Takizuka, K. Tani, M. Azumi and K. Shimizu, J. Nucl. Mater. **128** & **129**, 104 (1984).

[8]K. U. Riemann, Phys. Fluids B **1**, 961 (1989).

FIGURE CAPTIONS

Fig. 1. The geometry of the model and axial profiles of the potential and the magnetic field strength.

Fig. 2. The normalized potential profile in the presheath for the particle source with the spatial distribution (a) $h(s) = n(s)/n_0$ and (b) $h(s) = 1$. The model field b in Ref. 5 is used for the magnetic mirror profile. A dotted line is the analytical solution by Sato et al. for $h(s) = n(s)/n_0$, and a broken line is the simulation result by Hussein et al. for $h(s) = 1$.

Fig. 3. The normalized potential at the wall Ψ_w and that at the sheath edge Ψ_1 as a function of the mirror ratio at the sheath edge R_1 for the particle source with (a) $h(s) = n(s)/n_0$ and (b) $h(s) = 1$. The model field in Ref. 5 is used. Dotted lines are the analytical solutions for the particle source with $h(s) = n(s)/n_0$ by Sato et al., and broken lines are the simulation results for the particle source with $h(s) = 1$ by Hussein et al..

Fig. 4. The normalized potential profiles for the magnetic mirror ratio profile $R(s) = 1 + (R_1 - 1)s^2$ with $R_1 = 1.0$, 2.0, and 4.0, where the spatial distribution of the particle source is chosen as $h(s) = \exp(-25s^2)$.

Fig. 5. The profile of the normalized plasma density $n(s)/n_0$ for the magnetic mirror ratio $R_1 = 1.0$, 2.0, and 4.0.

Fig. 6. The normalized ion distribution function at the sheath edge for various values of R_1. The value $< V_{\|}^{-2} >$ is equal to 2.0 in the case of the uniform magnetic field and smaller than 2.0 in the case of the expanding magnetic field.

Fig. 7. The normalized potential profile for the partial source with the spatial distributions $h(s) = \exp(-25s^2)$ (——), $h(s) = 1$ (– – –), and $h(s) = \exp(-25(1-s)^2)$ (------). The magnetic mirror ratio profile is chosen as $R(s) = 1 + s^2$.

Fig. 8. The profile of the normalized plasma density $n(s)/n_0$ for the particle source with $h(s) = \exp(-25s^2)$(——), $h(s) = 1$(– – –), and $h(s) = \exp(-25(1-s)^2)$ (------).

Fig. 9. The normalized ion distribution function at the sheath edge for the particle source with $h(s) = \exp(-25s^2)$ (——), $h(s) = 1$ (– – –), and $h(s) = \exp(-25(1-s)^2)$ (------). The value $< V_{\|}^{-2} >$ is always smaller than 2.0.

Fig. 10. The upper and lower limits (—— and ------) of the normalized potential at the sheath edge, Ψ_1, and those of the potential at the wall, Ψ_w, as a function of the edge mirror ratio R_1. Bracken lines are results for the particle source with $h(s) = 1$.

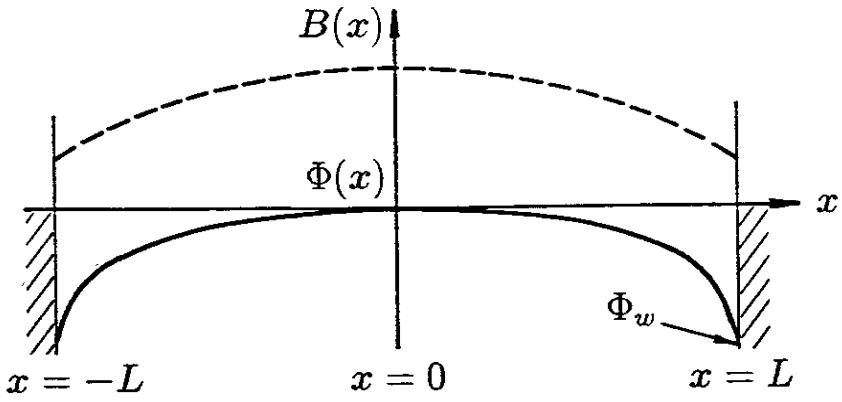
$B(x)$
$\Phi(x)$
x
Φ_w
$x=-L$
$x=0$
$x=L$

Fig. 1

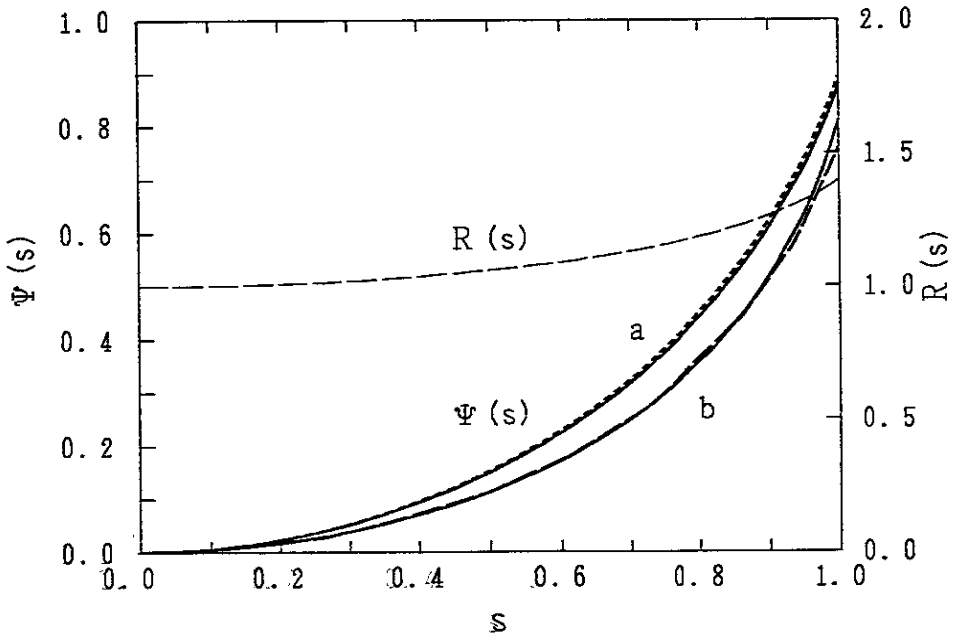
1.0
0.8
0.6
0.4
0.2
0.0
Ψ(s)
2.0
1.5
1.0
0.5
0.0
R(s)
R (s)
a
Ψ (s)
b
0.0
0.2
0.4
0.6
0.8
1.0
s

Fig. 2

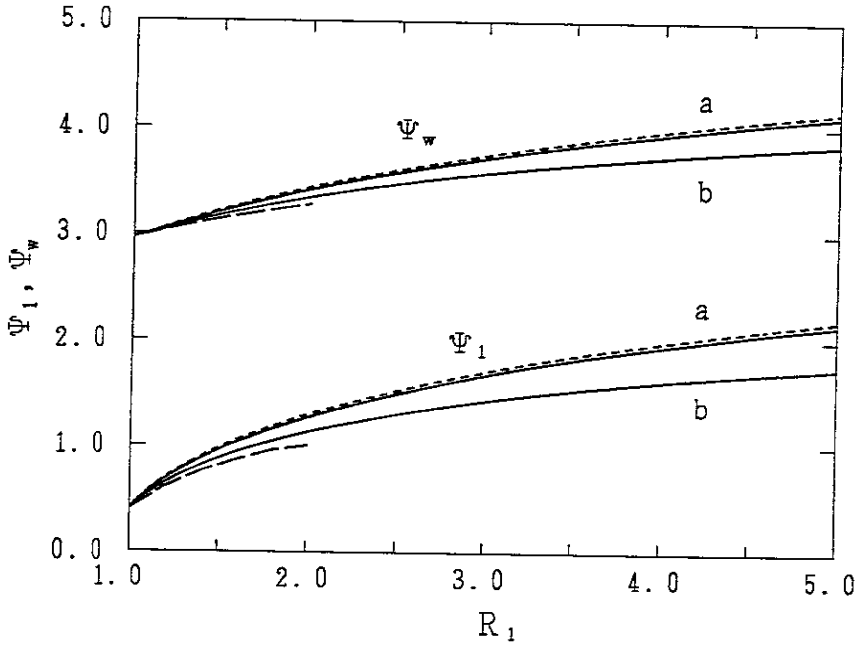
5.0
4.0
3.0
2.0
1.0
0.0
1.0
2.0
3.0
4.0
5.0
Ψ_1, Ψ_w
R_1
Ψ_w
Ψ_1
a
b
a
b

Fig. 3

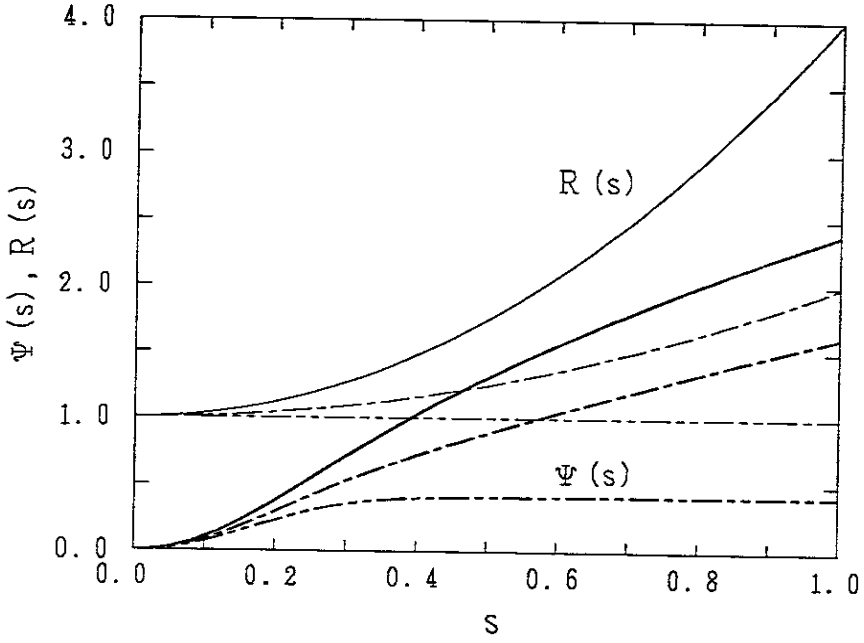
4.0
3.0
2.0
1.0
0.0
0.0
0.2
0.4
0.6
0.8
1.0
Ψ(s), R(s)
S
R(s)
Ψ(s)

Fig. 4

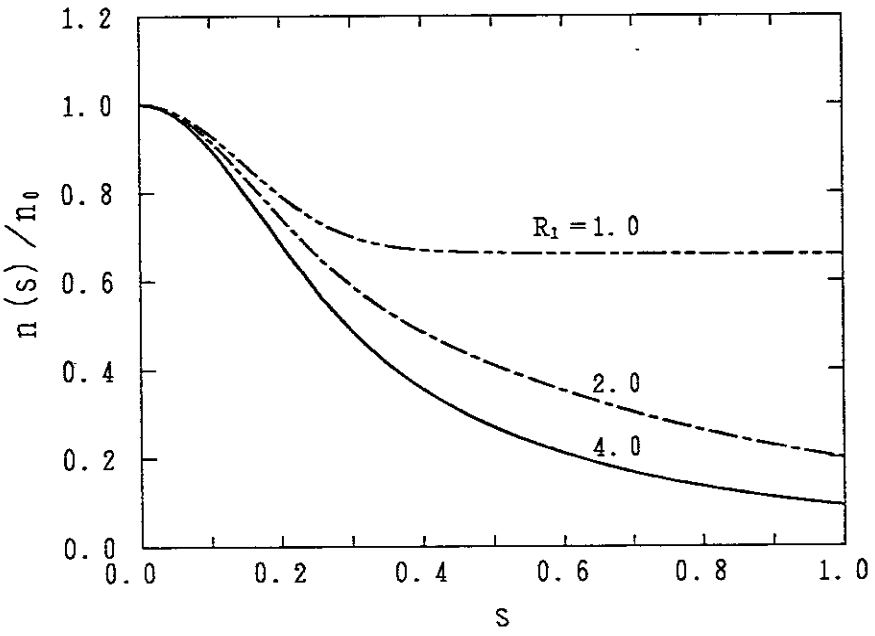
1.2
1.0
0.8
0.6
0.4
0.2
0.0
n(s)/n₀
R₁=1.0
2.0
4.0
0.0
0.2
0.4
0.6
0.8
1.0
S

Fig. 5

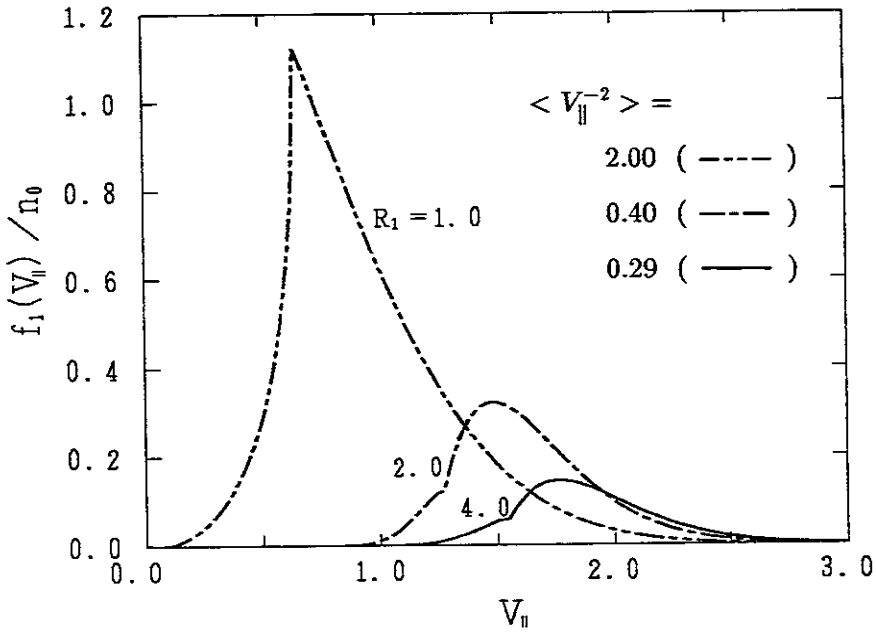
1.2
1.0
0.8
0.6
0.4
0.2
0.0
f₁(V∥)/n₀
< V∥⁻² > =
2.00 (----)
0.40 (— —)
0.29 (——)
R₁=1.0
2.0
4.0
0.0
1.0
2.0
3.0
V∥

Fig. 6

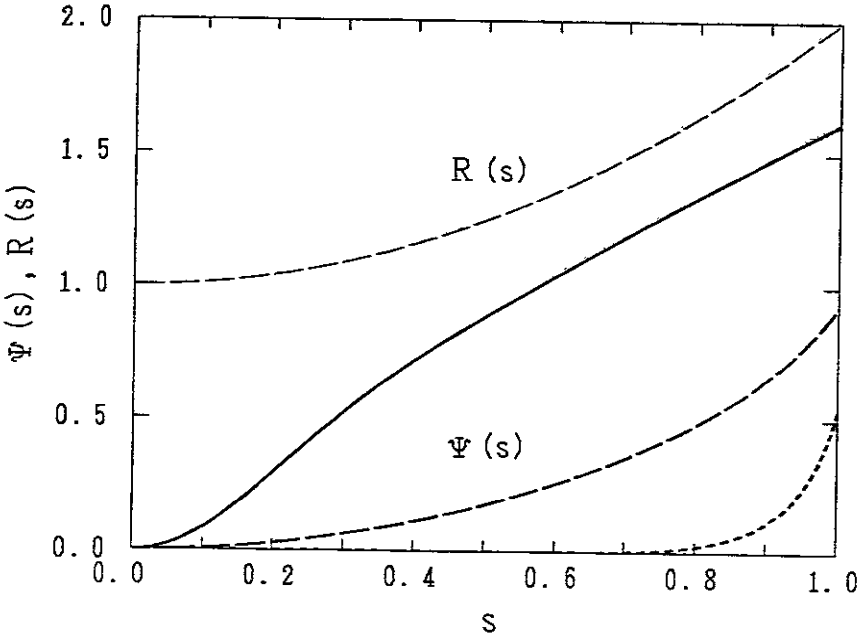
2.0
1.5
1.0
0.5
0.0
Ψ(s), R(s)
R(s)
Ψ(s)
0.0
0.2
0.4
0.6
0.8
1.0
S

Fig. 7

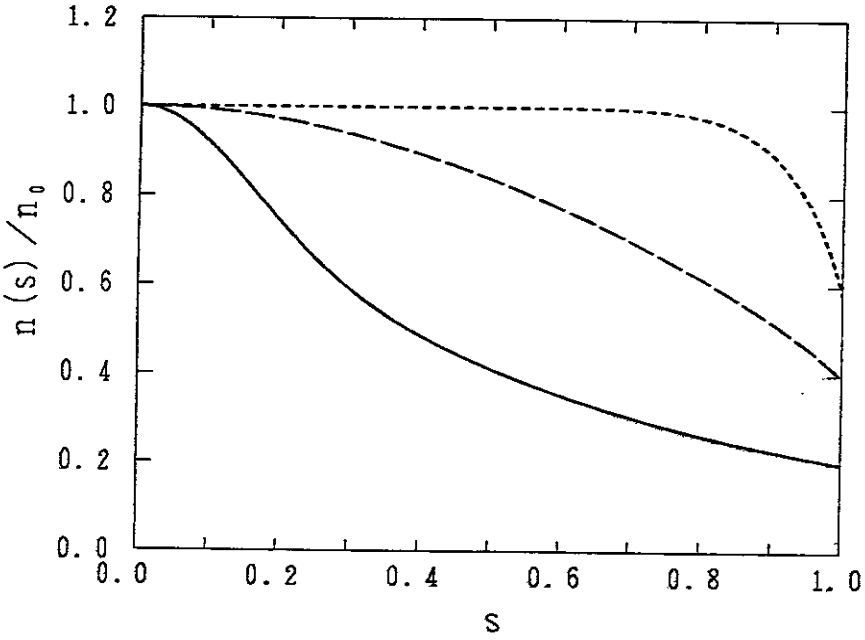
1.2
1.0
0.8
0.6
0.4
0.2
0.0
n(s)/n0
0.0
0.2
0.4
0.6
0.8
1.0
S

Fig. 8

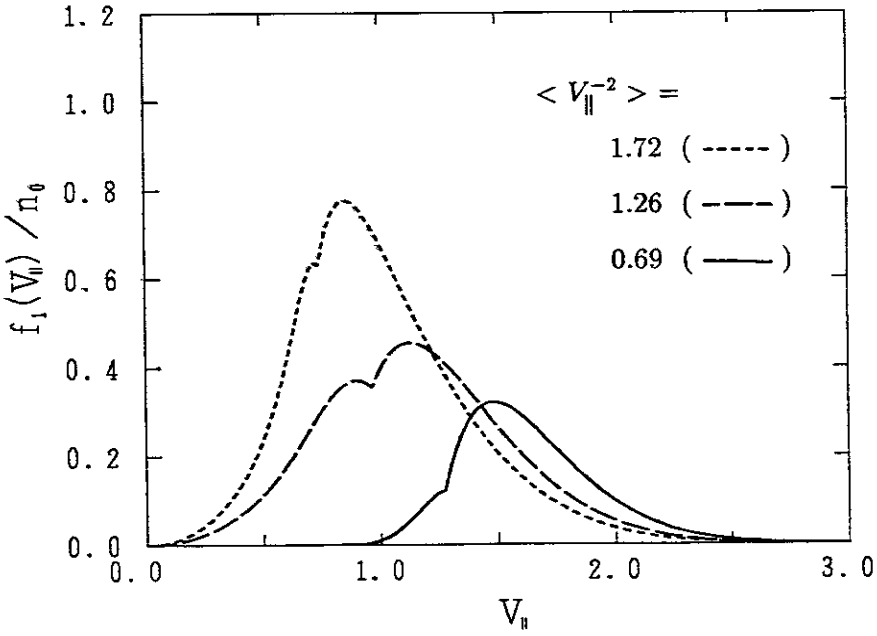
1.2
1.0
0.8
0.6
0.4
0.2
0.0
0.0
1.0
2.0
3.0
$f_1(V_\parallel) / n_0$
$V_\parallel$
$< V_\parallel^{-2} > =$
1.72 (-----)
1.26 (— — —)
0.69 (——)

Fig. 9

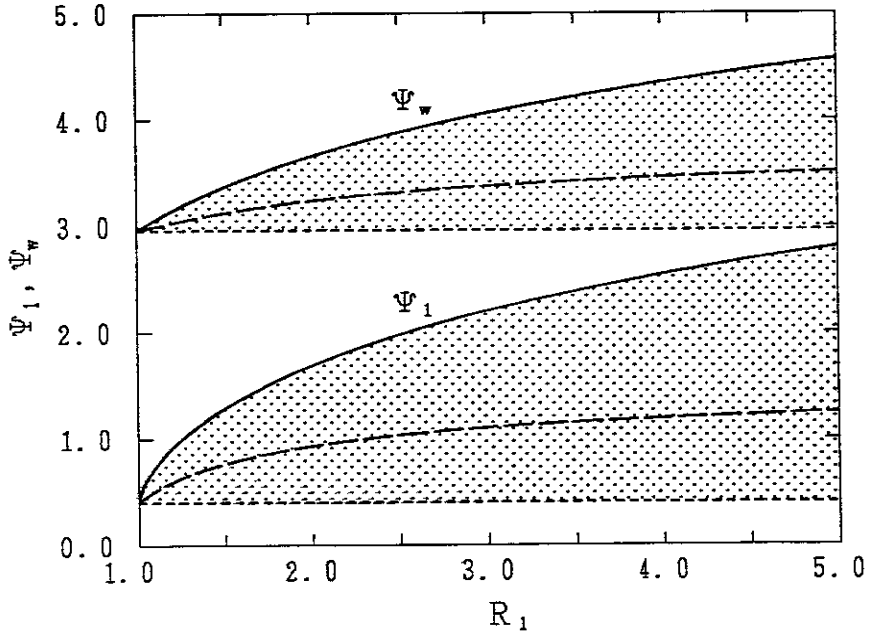
5.0
4.0
3.0
2.0
1.0
0.0
1.0
2.0
3.0
4.0
5.0
Ψ_1, Ψ_w
R_1
Ψ_w
Ψ_1

Fig. 10

Recent Issues of NIFS Series

NIFS-36 N. Ueda, S.-I. Itoh, M. Tanaka and K. Itoh, *A Design Method of Divertor in Tokamak Reactors* Aug. 1990

NIFS-37 J. Todoroki, *Theory of Longitudinal Adiabatic Invariant in the Helical Torus*; Aug. 1990

NIFS-38 S.-I. Itoh and K. Itoh, *Modelling of Improved Confinements – Peaked Profile Modes and H-Mode–* ; Sep. 1990

NIFS-39 O. Kaneko, S. Kubo, K. Nishimura, T. Syoji, M. Hosokawa, K. Ida, H. Idei, H. Iguchi, K. Matsuoka, S. Morita, N. Noda, S. Okamura, T. Ozaki, A. Sagara, H. Sanuki, C. Takahashi, Y. Takeiri, Y. Takita, K. Tsuzuki, H. Yamada, T. Amano, A. Ando, M. Fujiwara, K. Hanatani, A. Karita, T. Kohmoto, A. Komori, K. Masai, T. Morisaki, O. Motojima, N. Nakajima, Y. Oka, M. Okamoto, S. Sobhanian and J. Todoroki, *Confinement Characteristics of High Power Heated Plasma in CHS*; Sep. 1990

NIFS-40 K. Toi, Y. Hamada, K. Kawahata, T. Watari, A. Ando, K. Ida, S. Morita, R. Kumazawa, Y. Oka, K. Masai, M. Sakamoto, K. Adati, R. Akiyama, S. Hidekuma, S. Hirokura, O. Kaneko, A. Karita, T. Kawamoto, Y. Kawasumi, M. Kojima, T. Kuroda, K. Narihara, Y. Ogawa, K. Ohkubo, S. Okajima, T. Ozaki, M. Sasao, K. Sato, K.N. Sato, T. Seki, F. Shimpo, H. Takahashi, S. Tanahashi, Y. Taniguchi and T. Tsuzuki, *Study of Limiter H- and IOC- Modes by Control of Edge Magnetic Shear and Gas Puffing in the JIPP T-IIU Tokamak*; Sep. 1990

NIFS-41 K. Ida, K. Itoh, S.-I. Itoh, S. Hidekuma and JIPP T-IIU & CHS Group, *Comparison of Toroidal/Poloidal Rotation in CHS Heliotron/Torsatron and JIPP T-IIU Tokamak*; Sep .1990

NIFS-42 T.Watari, R.Kumazawa,T.Seki, A.Ando,Y.Oka, O.Kaneko, K.Adati, R.Ando, T.Aoki, R.Akiyama, Y.Hamada, S.Hidekuma, S.Hirokura, E.Kako, A.Karita, K.Kawahata, T.Kawamoto, Y.Kawasumi, S.Kitagawa, Y.Kitoh, M.Kojima, T. Kuroda, K.Masai, S.Morita, K.Narihara, Y.Ogawa, K.Ohkubo, S.Okajima, T.Ozaki, M.Sakamoto, M.Sasao, K.Sato, K.N.Sato, F.Shinbo, H.Takahashi, S.Tanahashi, Y.Taniguchi, K.Toi, T.Tsuzuki, Y.Takase, K.Yoshioka, S.Kinoshita, M.Abe, H.Fukumoto, K.Takeuchi, T.Okazaki and M.Ohtuka, *Application of Intermediate Frequency Range Fast Wave to JIPP T-IIU and HT-2 Plasma*; Sep. 1990

NIFS-43 K.Yamazaki, N.Ohyabu, M.Okamoto, T.Amano, J.Todoroki, Y.Ogawa, N.Nakajima, H.Akao, M.Asao, J.Fujita, Y.Hamada, T.Hayashi, T.Kamimura, H.Kaneko, T.Kuroda, S.Morimoto, N.Noda, T.Obiki, H.Sanuki, T.Sato, T.Satow, M.Wakatani, T.Watanabe, J.Yamamoto, O.Motojima, M.Fujiwara, A.Iiyoshi and LHD Design Group, *Physics Studies on Helical Confinement Configurations with l=2 Continuous Coil Systems*; Sep. 1990

NIFS-44 T.Hayashi, A.Takei, N.Ohyabu, T.Sato, M.Wakatani, H.Sugama, M.Yagi, K.Watanabe, B.G.Hong and W.Horton, *Equilibrium Beta Limit and Anomalous Transport Studies of Helical Systems*; Sep. 1990

NIFS-45 R.Horiuchi, T.Sato, and M.Tanaka, *Three-Dimensional Particle Simulation Study on Stabilization of the FRC Tilting Instability*; Sep. 1990

NIFS-46 K.Kusano, T.Tamano and T. Sato, *Simulation Study of Nonlinear Dynamics in Reversed-Field Pinch Configuration*; Sep. 1990

NIFS-47 Yoshi H.Ichikawa, *Solitons and Chaos in Plasma*; Sep. 1990

NIFS-48 T.Seki, R.Kumazawa, Y.Takase, A.Fukuyama, T.Watari, A.Ando, Y.Oka, O.Kaneko, K.Adati, R.Akiyama, R.Ando, T.Aoki, Y.Hamada, S.Hidekuma, S.Hirokura, K.Ida, K.Itoh, S.-I.Itoh, E.Kako, A. Karita, K.Kawahata, T.Kawamoto, Y.Kawasumi, S.Kitagawa, Y.Kitoh, M.Kojima, T.Kuroda, K.Masai, S.Morita, K.Narihara, Y.Ogawa, K.Ohkubo, S.Okajima, T.Ozaki, M.Sakamoto, M.Sasao, K.Sato, K.N.Sato, F.Shinbo, H.Takahashi, S.Tanahashi, Y.Taniguchi, K.Toi and T.Tsuzuki, *Application of Intermediate Frequency Range Fast Wave to JIPP T-IIU Plasma*; Sep.1990

NIFS-49 A.Kageyama, K.Watanabe and T.Sato, *Global Simulation of the Magnetosphere with a Long Tail: The Formation and Ejection of Plasmoids*; Sep.1990

NIFS-50 S.Koide, *3-Dimensional Simulation of Dynamo Effect of Reversed Field Pinch*; Sep. 1990

NIFS-51 O.Motojima, K. Akaishi, M.Asao, K.Fujii, J.Fujita, T.Hino, Y.Hamada, H.Kaneko, S.Kitagawa, Y.Kubota, T.Kuroda, T.Mito, S.Morimoto, N.Noda, Y.Ogawa, I.Ohtake, N.Ohyabu, A.Sagara, T. Satow, K.Takahata, M.Takeo, S.Tanahashi, T.Tsuzuki, S.Yamada, J.Yamamoto, K.Yamazaki, N.Yanagi, H.Yonezu, M.Fujiwara, A.Iiyoshi and LHD Design Group, *Engineering Design Study of Superconducting Large Helical Device*; Sep. 1990

NIFS-52 T.Sato, R.Horiuchi, K. Watanabe, T. Hayashi and K.Kusano, *Self-Organizing Magnetohydrodynamic Plasma*; Sep. 1990

NIFS-53 M.Okamoto and N.Nakajima, *Bootstrap Currents in Stellarators and Tokamaks*; Sep. 1990

NIFS-54 K.Itoh and S.-I.Itoh, *Peaked-Density Profile Mode and Improved Confinement in Helical Systems*; Oct. 1990

NIFS-55 Y.Ueda, T.Enomoto and H.B.Stewart, *Chaotic Transients and Fractal Structures Governing Coupled Swing Dynamics*; Oct. 1990

NIFS-56 H.B.Stewart and Y.Ueda, *Catastrophes with Indeterminate Outcome*; Oct. 1990

NIFS-57 S.-I.Itoh, H.Maeda and Y.Miura, *Improved Modes and the Evaluation of Confinement Improvement*; Oct. 1990

NIFS-58 H.Maeda and S.-I.Itoh, *The Significance of Medium- or Small-size Devices in Fusion Research*; Oct. 1990

NIFS-59 A.Fukuyama, S.-I.Itoh, K.Itoh, K.Hamamatsu, V.S.Chan, S.C.Chiu, R.L.Miller and T.Ohkawa, *Nonresonant Current Drive by RF Helicity Injection*; Oct. 1990

NIFS-60 K.Ida, H.Yamada, H.Iguchi, S.Hidekuma, H.Sanuki, K.Yamazaki and CHS Group, *Electric Field Profile of CHS Heliotron/Torsatron Plasma with Tangential Neutral Beam Injection*; Oct. 1990

NIFS-61 T.Yabe and H.Hoshino, *Two- and Three-Dimensional Behavior of Rayleigh-Taylor and Kelvin-Helmholz Instabilities*; Oct. 1990

NIFS-62 H.B. Stewart, *Application of Fixed Point Theory to Chaotic Attractors of Forced Oscillators;* Nov. 1990

NIFS-63 K.Konn., M.Mituhashi, Yoshi H.Ichikawa,*Soliton on Thin Vortex Filament;* Dec. 1990

NIFS-64 K.Itoh, S.-I.Itoh and A.Fukuyama,*Impact of Improved Confinement on Fusion Research;* Dec. 1990

NIFS -65 A.Fukuyama, S.-I.Itoh and K. Itoh,*A Consistency Analysis on the Tokamak Reactor Plasmas;* Dec. 1990

NIFS-66 K.Itoh, H. Sanuki, S.-I. Itoh and K. Tani,*Effect of Radial Electric Field on α-Particle Loss in Tokamaks;* Dec. 1990

NIFS DATA-1 Y. Yamamura, T. Takiguchi and H. Tawara, *Data Compilation of Angular Distributions of Sputtered Atoms* ; Jan. 1990

NIFS DATA-2 T. Kato, J. Lang and K. E. Berrington, *Intensity Ratios of Emission Lines from OV Ions for Temperature and Density Diagnostics* ; Mar. 1990

NIFS DATA-3 T. Kaneko, *Partial Electronic Straggling Cross Sections of Atoms for Protons* ; Mar. 1990

NIFS DATA-4 T. Fujimoto, K. Sawada and K. Takahata, *Cross Section for Production of Excited Hydrogen Atoms Following Dissociative Excitation of Molecular Hydrogen by Electron Impact* ; Mar. 1990

NIFS DATA-5 H. Tawara, *Some Electron Detachment Data for H- Ions in Collisions with Electrons, Ions, Atoms and Molecules – an Alternative Approach to High Energy Neutral Beam Production for Plasma Heating–* ; Apr. 1990

NIFS DATA-6 H. Tawara, Y. Itikawa, H. Nishimura, H. Tanaka and Y. Nakamura, *Collision Data Involving Hydro-Carbon Molecules* ; July 1990

NIFS DATA-7 H.Tawara, *Bibliography on Electron Transfer Processes in Ion-Ion/Atom/Molecule Collisions –Updated 1990–*; Oct. 1990

NIFS DATA-8 U.I.Safronova, T.Kato, K.Masai, L.A.Vainshtain and A.S.Shlyapzeva, *Excitation Collision Sterengths, Cross Scetions and Rate Coefficients for OV, SiXI, FeXXIII, MoXXXIX by Electron Impact($1s^2 2s^2$-$1s^2 2s2p$-$1s^2 2p^2$ Transitions)*

NIFS DATA-9 T.Kaneko, *Partial and Total Electronic Stopping Cross Sections of Atoms and Solids for Protons;* Dec 1990

NIFS TECH-1 H. Bolt and A. Miyahara, *Runaway–Electron –Materials Interaction Studies* ; Mar. 1990

NIFS PROC-1 *U.S.-Japan Workshop on Comparison of Theoretical and Experimental Transport in Toroidal Systems Oct. 23-27, 1989* ; Mar. 1990

NIFS PROC-2 *Structures in Confined Plasmas –Proceedings of Workshop of US-Japan Joint Institute for Fusion Theory Program–* ; Mar. 1990

NIFS PROC-3 *Proceedings of the First International Toki Conference on Plasma Physics and Controlled Nuclear Fusion –Next Generation Experiments in Helical Systems– Dec. 4-7, 1989* ; Mar. 1990

NIFS PROC-4 *Plasma Spectroscopy and Atomic Processes –Proceedings of the Workshop at Data & Planning Center in NIFS–*; Sep. 1990

NIFS PROC-5 *Symposium on Development of Intensed Pulsed Particle Beams and Its Applications*; Oct. 1990